

## Rate of cation disordering in orthopyroxenes

JAMES R. BESANCON

Department of Geology  
Wellesley College  
Wellesley, Massachusetts 02181

### Abstract

Isothermal cation disordering experiments at 600–800°C on two orthopyroxenes, followed by Mössbauer spectroscopy to determine iron intersite partitioning, give rates consistent with a second-order kinetic model. The characteristic disordering rate constant for Fe–Mg exchange  $K(21) = 2.8 \times 10^{-3} \text{ min}^{-1}$  for a magnesian pyroxene, but  $1.5 \times 10^{-2} \text{ min}^{-1}$  for a more iron-rich sample. Activation energies are 260 and 254 kJ/mole, respectively. Predicted attainment of equilibrium is about 14 weeks at 500°C for one orthopyroxene and one second at 1000°C for the other; this suggests that previous 500°C distribution data may have failed to reach equilibrium in two week runs, and that 1000°–1300°C data may be suspect because the high temperature distributions are unquenchable. A two-stage model for ordering, with some cut-off temperature below which the ordering mechanism changes, is probably unnecessary to explain naturally-occurring pyroxene disorder because the activation energies reported here indicate a rather drastic slowing of rates at lower temperatures.

### Introduction

Divalent magnesium and iron ions are found in two nonequivalent six-coordinated crystallographic sites in orthopyroxene. In all known samples, iron is preferentially ordered into the more distorted M2 site, and magnesium into the more regular octahedral M1 site (Ghose, 1965, and many subsequent workers); however, neither complete order nor complete disorder is found. Greater ordering is observed in metamorphic and plutonic rocks, less in volcanic rocks.

Cation ordering in orthopyroxenes was once investigated as a possible geothermometer, but heating studies (Virgo and Hafner, 1969, 1970) showed apparent  $\text{Mg}^{2+}$ – $\text{Fe}^{2+}$  equilibration temperatures of 500°–600°C for natural igneous samples, and lower apparent temperatures for metamorphic samples, too low to be crystallization temperatures. Re-equilibration is a relatively rapid process, and occurs to fairly low temperatures. On the other hand, rapid rates of cation exchange may make possible the investigation of relatively rapid cooling at higher temperatures (e.g., volcanic eruptions, Johnston, 1979) or, by extrapolation, to slower cooling at lower temperatures (e.g., studies of anthophyllite by Seifert and Virgo,

1974, 1975, and of orthopyroxenes by Khisina *et al.*, 1976).

In order to determine quantitative cooling rates, appropriate models of equilibrium distribution and ordering rate must be determined, and their generality tested. The present investigation is aimed at measuring disordering rates because greater analytical precision is possible than for ordering studies; further work is underway to determine ordering rates. Many of the factors that influence disordering rates should have the same effect on ordering rates; factors include fugacities of various species (especially oxygen), bulk composition, inhomogeneity, shear and exsolution lamellae, general defect structure of the crystals, and experimental errors.

An effective model of the equilibrium distribution of Mg and Fe between sites should allow the site populations to be predicted for any composition, pressure, and temperature. As little pressure dependence is expected for cations with such similar sizes, and none was found by Virgo and Hafner (1969), the most important factors are apparently bulk composition and temperature. For a single sample with  $\text{Fe}/(\text{Fe}+\text{Mg}) = 0.574$  and at temperatures between 600° and 1000°C, Virgo and Hafner obtained a relatively constant molar Gibbs free energy of intracrystalline

exchange

$$\Delta G = -RT \ln K_D \quad (1)$$

where:

$$K_D = \frac{[X(\text{FeM1})][1 - X(\text{FeM2})]}{[X(\text{FeM2})][1 - X(\text{FeM1})]} \quad (2)$$

and  $X(\text{AB})$  is the mole fraction of ion A in site B at equilibrium. It should be noted that Mueller (1967, 1969) used  $X\text{MgM1}$  for his variable  $X1$ , resulting in values the reciprocal of this  $K_D$ . As pointed out by Navrotsky (1971), this free energy term is actually a combination of the enthalpy and non-configurational (lattice-vibrational) entropy. The tendency of Fe to order into the M2 site is partially offset by the configurational entropy, which favors mixing.

Systematic studies of samples of differing composition by Saxena and Ghose (1971) and Saxena (1973) showed that a more complex solution theory is needed to account for variations arising from differing bulk compositions. For a temperature range of 500–800°C, they used an equation of the form:

$$\ln K = \ln K_D + \frac{W(\text{M1})}{RT} [1 - 2X(\text{FeM1})] - \frac{W(\text{M2})}{RT} [1 - 2X(\text{FeM2})] \quad (3)$$

where the  $W$  terms are parameters used with  $K$  to fit values of  $K_D$  at different compositions and temperatures. An alternate form based on a virial expansion, given by Thompson (1969, 1970) may also be used (Sack, 1980, and Grover, 1980), with certain advantages in calculating consistent interphase distributions. Analysis of data on orthopyroxenes with bulk  $\text{Fe}/(\text{Fe}+\text{Mg}) = 0.181$  to  $0.86$  by Saxena and Ghose (1971) gave internally consistent results for temperatures of 600°, 700°, and 800°C, but some discrepancy at 500°C. They noted that small errors in site occupancy determinations would make relatively large changes in  $W(\text{M1})$  and  $W(\text{M2})$  at 500°C and Saxena (1973) gave linear extrapolations from higher temperatures for  $K$ ,  $W(\text{M1})$ , and  $W(\text{M2})$  at 500°C.

While nonideal solution models such as those of Saxena and Ghose (1971) and Sack (1980) are convenient because they allow extrapolated apparent equilibration temperatures for all binary compositions, a formulation by Seifert (1978) is particularly useful in analyzing individual samples because a more accurate estimate of the temperature variation of the standard free energy of exchange for a natural sample can be made. By determining equilibrium

distributions at several temperatures on a sample, the extrapolation to lower temperatures takes into account any bias that might be introduced by the presence of components in the formula not on the binary join enstatite-ferrosilite. Seifert defines a non-configurational free energy like that of Virgo and Hafner (1969)

$$\Delta G = -RT \ln K_D \quad (4)$$

Using the formula

$$\Delta G = \Delta H - T\Delta S \quad (5)$$

an enthalpy and excess entropy can be found. Then equation 6 can be used to estimate apparent equilibration temperatures from the distribution in natural samples.

$$T_{ae} = \frac{\Delta H}{\Delta S - R \ln K_D} \quad (6)$$

Several models have been proposed for the kinetics of the ordering and disordering process. Mueller (1967, 1969) derived an integrated equation for change of the state of order with time based on second-order kinetics, which was used by Virgo and Hafner (1969) to analyze their sparse disordering and ordering rate data and to obtain rate constants and an activation energy for disordering:

$$K(21)\Delta t = \frac{K_D}{2d} \left[ \ln \frac{(d-f)}{(d+f)} \right] \frac{X(\text{FeM2})''}{X(\text{FeM2})'} \quad (7)$$

where

$$f = \left[ cX(\text{FeM2}) + \frac{b}{2} \right],$$

$$d = \left( \frac{b^2}{4} - ca \right)^{1/2},$$

$$c = 1 - K_D,$$

$$b = 2K_D X - 2X - K_D - 1,$$

$$a = 2X,$$

$X$  = bulk mole fraction of Fe, assumed in the absence of site distribution data for other cations to be  $\text{Fe}/(\text{Fe}+\text{Mg})$ ,

$X(\text{FeM2})'$  = the initial value of  $X(\text{FeM2})$ , and

$X(\text{FeM2})''$  is the site population at the end of the heating experiment, for times insufficient to allow attainment of equilibrium.

$\Delta t$  = the duration of heating experiment.

This version of the equation incorporates a  $1/2 C_0$  factor (expressing the concentration of sites and assumed constant if ordered and disordered crystals

have the same unit cell volume) into  $K(21)$ , and assumes that the nonideality coefficients (analogous to activity coefficients) are all unity, as present data are not accurate enough to warrant other procedures. It should be noted that Mueller's derivation used  $X_{MgM1}$  as the variable, which results in  $K(12)$  being the disordering rate constant, rather than  $K(21)$  as used by Virgo and Hafner (1969) and in this work. Khristoforov *et al.* (1974) rejected Mueller's model for their data on disordering rate at 500°, 700°, and 900°C, and proposed a first-order kinetic model with a first stage characterized by rapid disordering followed by a second stage with much slower disordering. However, their data are reasonably fitted (Fig. 1) by the Mueller equation for isothermal disordering when proper values of  $K(21)$ , the rate constant, and  $K_D$ , the distribution coefficient at equilibrium, are chosen.

As will be shown below, some equilibrium values at 500°C and below, and 900°C and above, may be suspect; in addition, data from incomplete disordering experiments are sparse at all temperatures. These factors cast doubt on published determinations of rate constants and activation energies.

The Mueller model will be used here to systematize the rate of disordering of two different orthopyroxenes; results will be used to estimate equilibrium values.

### Experimental

Two samples from metamorphic rocks were chosen, to provide highly ordered pyroxenes in large quantities. Samples were ground and sieved to 35–60 mesh (to minimize high-diffusivity paths on surfaces), and separations were done with heavy liquids and magnetic separator. Some impurities remained in both samples, as revealed by optical, electron microscope, and X-ray diffraction analysis. In sample HC, separated from a pyroxenite from Harford County, Maryland, minor chromite, anthophyllite, augite, and serpentine were present; there were no apparent effects on the Mössbauer spectra, with the possible exception that there might be very small contributions to peak areas of the pyroxene from the anthophyllite which would not be visible because of the close overlap in peak position. Sample TZ, from a Tanzanian granulite gneiss, with modal hypersthene, plagioclase, augite, hornblende, and magnetite, contains the latter three as minor iron-bearing impurities, with small effects on the Mössbauer spectra. The orthopyroxenes themselves were chosen to be as close to binary mixtures of enstatite and fer-

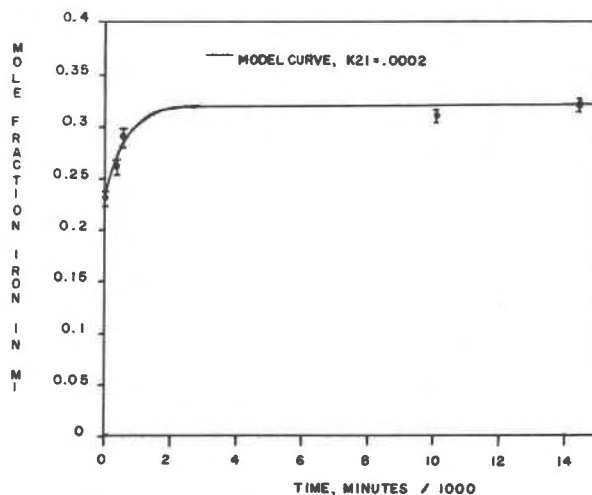


Fig. 1. Data of Khristoforov *et al.* (1974) at 500°C, fit to the kinetic model of Mueller (1967,1969). With the appropriate value of  $K(21)$ , the rate constant, the model fits the data reasonably well.

rosilite as possible. A special attempt was made to choose samples low in calcium and aluminum, which may strongly affect the Mössbauer spectra. Compositions (Table 1) were determined using the MAC automated electron microprobe at Massachusetts Institute of Technology, and were found to be homogeneous.

Samples of 150 mg were loaded into platinum capsules crimped closed except for a small opening at the top, and suspended from platinum wires. A gas-mixing apparatus (Nafziger *et al.*, 1971, and A. Duba, personal communication) provided an  $H_2$ - $CO_2$  atmosphere in an attempt to control the oxygen fugacity around the samples, as diffusion rates, espe-

Table 1. Chemical composition of samples

Sample:	HC		TZ	
	Wt. %	Mol. prop.	Wt. %	Mol. prop.
MgO	32.42	1.702	16.07	0.936
FeO*	8.74	0.257	30.34	0.992
SiO <sub>2</sub>	55.65	1.960	49.68	1.944
CaO	0.59	0.021	0.70	0.028
Al <sub>2</sub> O <sub>3</sub>	1.07	0.043	1.59	0.074
MnO	0.22	0.006	1.01	0.034
Na <sub>2</sub> O	0.02	0.001	0.00	0.000
TiO <sub>2</sub>	0.11	0.002	0.09	0.002
Cr <sub>2</sub> O <sub>3</sub>	0.41	0.011	0.03	0.000
Total	99.22	4.004	99.52	4.010

\*All Fe as FeO

Mole proportions are cations per six oxygens.

cially in iron-bearing minerals (Buening and Buseck, 1973), may be altered by variation in the partial pressure of anions around the sample. A furnace with a 46 cm heated zone was used in an attempt to promote equilibrium between the two gases at the low temperatures (600–900°C) of this study. Accuracy was checked at 900°C against the iron-wustite buffer, but no attempt was made to determine whether equilibrium was reached at lower temperatures. Quenching was by mechanical release and 60 cm drop into mercury or water, which gave apparently identical results.

Samples were heated in two different ways, depending on the projected length of the run. For short heating times, single samples were drawn up into a preheated furnace with gases flowing, held a pre-determined time, and quenched. Samples reached set temperature in one minute or less. For longer heating times, seven samples were loaded in radially symmetric positions into a cold furnace, gases started, and temperature run up in about 30 minutes. One sample was quenched immediately and used as the initial value  $X(\text{FeM2})$  for disordering rate calculations, to eliminate any bias that might result from changes occurring during warmup. In the data (Table 2) multiple sample runs have a value of  $t(\text{adj.})$  (adjusted time) about 30 minutes less than  $t(\text{total})$ , while single run samples are only one minute less than  $t(\text{total})$ . These adjusted times are used for all calculations and figures.

Temperatures were monitored with a Chromel-Alumel thermocouple calibrated against the melting points of gold and sodium chloride, and placed in a position symmetric to the sample positions, at the hot spot of the furnace. The variation from top to bottom of the sample was 1°C outside the capsule, and presumably less inside. Control of temperature is estimated at  $\pm 3^\circ\text{C}$  overall.

Fe Mössbauer spectra were recorded in 512 channels of about 0.02 mm/sec/channel velocity increment each, and calibrated against iron foil. Samples were held at about 77°K with a liquid nitrogen-styrofoam cryostat to aid in resolution of peaks. Average run duration was 24 hours, typically with  $4-8 \times 10^5$  baseline counts per channel. Many samples were run in duplicate, denoted by an extra digit in the sample number of Table 2. Spectra were fitted to two doublets (HC) or three doublets (TZ) using a program fitting Lorentzian lineshapes with the Gauss non-linear method (Stone *et al.*, 1971). For sample HC, no constraints were placed on the peaks; for TZ, two peaks attributed to  $\text{Fe}^{3+}$  were constrained to be equal

Table 2. Fe distribution as a function of temperature and duration of heating

Sample	T°C	t, min	t, adj.	%Fe <sup>3+</sup>	%FeM1	XFeM1	-logf <sub>02</sub>
TZ164	600	2.0	1.0	9.48	14.48	0.1646	23.9
TZ150	600	138.0	120.0	9.98	18.26	0.2087	23.9
TZ160	600	258.0	240.0	13.14	19.16	0.2270	23.9
TZ161	600	378.0	360.0	11.90	18.74	0.2189	23.9
TZ162	600	498.0	480.0	11.56	19.51	0.2270	23.9
TZ147e	600	1220.0	1200.0	8.06	22.34	0.2500	23.9
TZ148e	600	1820.0	1800.0	7.40	21.59	0.2399	23.9
TZ149e	600	2420.0	2400.0	10.12	21.89	0.2506	23.9
TZ150e	600	3290.0	3270.0	9.72	22.05	0.2513	23.9
TZ130	700	2.0	1.0	6.58	8.01	0.0882	20.7
TZ131	700	5.0	4.0	6.36	9.98	0.1097	20.7
TZ132	700	10.5	9.5	7.42	13.09	0.1457	20.7
TZ133	700	15.0	14.0	6.54	13.34	0.1469	20.7
TZ133,2	700	15.0	14.0	6.60	13.69	0.1508	20.7
TZ154	700	25.0	24.0	8.78	24.50	0.2764	20.7
TZ157	700	25.0	24.0	10.38	23.63	0.2713	20.7
TZ157,2	700	25.0	24.0	10.08	22.72	0.2600	20.7
TZ158	700	30.0	29.0	11.34	21.88	0.2539	20.7
TZ138e	700	90.0	89.0	8.24	25.06	0.2802	20.7
TZ137e	700	165.0	164.0	6.46	26.09	0.2866	20.7
TZ142	750	2.0	1.0	11.46	19.40	0.2251	19.4
TZ143	750	4.0	3.0	8.72	25.45	0.2894	19.4
TZ145	750	6.0	5.0	9.98	25.39	0.2904	19.4
TZ146	750	8.0	7.0	10.58	25.17	0.2898	19.4
TZ144e	750	370.0	369.0	8.08	26.07	0.2907	19.4
TZ155	800	1.0	0.0	6.50	11.38	0.1252	18.2
TZ141	800	2.0	1.0	9.08	25.88	0.2929	18.2
TZ118e	800	4.0	3.0	8.14	28.05	0.3137	18.2
TZ119e	800	6.0	5.0	6.34	29.26	0.3213	18.2
TZ120e	800	8.0	7.0	7.64	28.25	0.3142	18.2
TZHP	Unheated			5.58	14.11	0.1411	----
HC1	Unheated			-----	10.03	0.0263	----
HC2	Unheated			-----	10.39	0.0273	----
HC3	Unheated			-----	10.24	0.0269	----
HC4	Unheated			-----	9.82	0.0258	----
HC4,2	Unheated			-----	10.78	0.0283	----
HC5	Unheated			-----	9.98	0.0262	----
HC37	700	31.5	0.0	-----	10.91	0.0286	22.2
HC38	700	55.0	23.5	-----	15.50	0.0407	22.2
HC39	700	145.0	113.5	-----	20.40	0.0535	22.2
HC40	700	350.0	318.5	-----	21.57	0.0565	22.2
HC41e	700	1260.0	1228.5	-----	24.08	0.0632	22.2
HC42e	700	1545.0	1513.5	-----	23.49	0.0616	22.2
HC43e	700	4180.0	4148.5	-----	23.98	0.0629	22.2
HC53	750	36.5	0.0	-----	16.57	0.0435	21.0
HC54	750	96.5	60.0	-----	26.06	0.0684	21.0
HC55e	750	174.0	137.5	-----	26.68	0.0702	21.0
HC56e	750	310.0	273.5	-----	26.24	0.0689	21.0
HC58e	750	1830.0	1793.5	-----	27.22	0.0714	21.0
HC35	800	5.0	5.0	-----	24.18	0.0634	19.8
HC34	800	12.0	12.0	-----	27.44	0.0720	19.8
HC36	800	20.0	20.0	-----	28.16	0.0739	19.8
HC20	800	44.0	6.0	-----	26.38	0.0692	19.8
HC21	800	120.0	82.0	-----	29.33	0.0770	19.8
HC22	800	198.0	160.0	-----	28.40	0.0745	19.8
HC23	800	280.0	242.0	-----	28.64	0.0752	19.8
HC24	800	608.0	570.0	-----	26.25	0.0689	19.8
HC25	800	1353.0	1315.0	-----	27.53	0.0722	19.8
HC26	800	2186.0	2148.0	-----	25.89	0.0679	19.8

Samples numbers ending in "e" were assumed to have reached equilibrium. The notation ",2" indicates duplicate Mossbauer spectrum of same sample.

in width and area, while other peaks were unconstrained. Site populations of iron were estimated using area ratios of M1 and M2 peaks. Following Saxena and Ghose (1971), the ratio  $\text{Fe}^{2+}/(\text{Fe}^{2+}+\text{Mg}^{2+})$  was calculated for each sample. For TZ, the microprobe analysis and charge and site stoichiometry considerations suggested that  $\text{Fe}^{3+}$  was less than 2% of total iron and only the M1 and M2 peaks are used. Some of the Mössbauer ferric doublet arises from

sample impurity; a hand-picked sample (TZHP) shows a reduction but not elimination of the ferric doublet, indicating that significant amounts of  $Fe^{3+}$  also substitute in the pyroxene. Treatment of the ferric iron as an impurity introduces small errors into the calculated  $K_D$ , but it is still in good agreement with other metamorphic pyroxenes of similar composition (Virgo and Hafner, 1970); distributions in heated samples of TZ agree (Fig. 2) with 600–800°C samples of Saxena and Ghose (1971).

With the above procedures, Mössbauer spectra of ten replicates of unheated sample TZ (two separate samples run six and four times, respectively), and six replicates of unheated sample HC (5 separate samples) were run. Standard deviations of mole fraction iron in M1 were 0.0165 (TZ) and 0.0009 (HC). The large scatter in sample TZ is due to the large total average mole fraction, to impurities in the sample, to lower average counts per channel in the Mossbauer spectra (typically 400,000 vs. 600,000), and to a larger number of runs (obviously, a very low number of samples, while giving the sample variance, gives less than the true population variance). Using Student's *t* statistic to obtain 90% confidence limits for the estimated standard deviation of the population of all possible runs, multipliers of 2.015 (for 6 samples) or 1.833 (for 10 samples) were used, giving error limits of  $\pm 0.0018$  (HC) and  $\pm 0.03$  (TZ). These are generous error estimates, as more highly disordered samples

are resolved more readily by the Mössbauer spectrometer. (As an example, 90% confidence limits derived from four equilibrium determinations at 600°C (Sample TZ) are  $\pm 0.013$ .) In some cases, samples were run in duplicate and both results used in the calculations. Error bars in Figures 3 and 4 used 90% confidence limits derived from the unheated samples. Impurities in TZ and HC may add small amounts to the areas of some peaks, which in turn may slightly affect the accuracy of the determinations of the inter-site distribution. However,  $K_D$  is in good agreement with that of previous workers as noted above, and the effect on calculated rate constants is negligible.

Results

Site populations for ferrous iron in the M1 site are presented in Table 2. The first column gives sample number, with an extra digit denoting duplicate Mössbauer spectra, and prefix letters denoting sample (HC or TZ). The third column gives total heating time, with the fourth column an "adjusted time" based on measured difference from the shortest run time. Samples used for rate constant calculations were all handled in the same manner (loaded into hot or cold furnace) for a given temperature, except TZ at 600°C. The shortest time sample was loaded into a preheated furnace, while the others were loaded cold and temperature was then increased. Runup time is short compared to that of the duration of the experiment.

The hydrogen-carbon dioxide gas mix used for sample HC was approximately 16%  $CO_2$  for all data

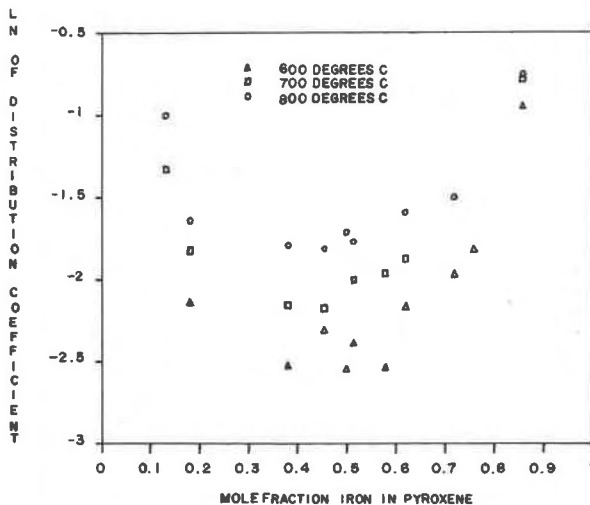


Fig. 2. Mole fraction  $X = Fe/(Fe+Mg)$  plotted against  $\ln(K_D)$ . Data for sample TZ at  $X = 0.51$ , sample HC at  $x = 0.13$ , other data from Saxena and Ghose (1971). These equilibria form a trend which is more symmetric about  $X = 0.5$  than the original curves of Saxena and Ghose because of the relatively disordered distributions in sample HC.

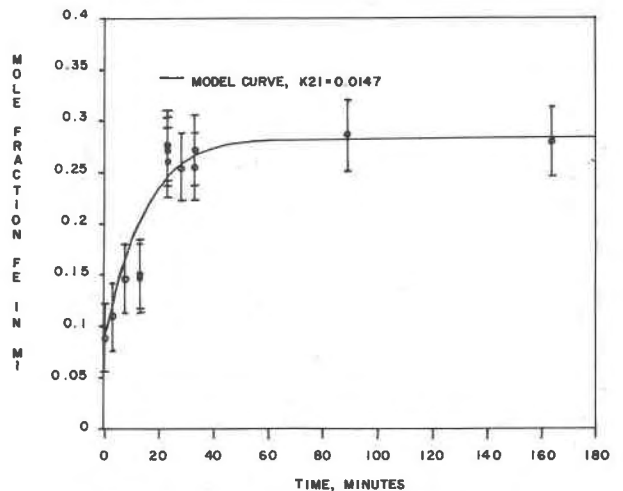


Fig. 3. Disordering with time at 700°C, Sample TZ.

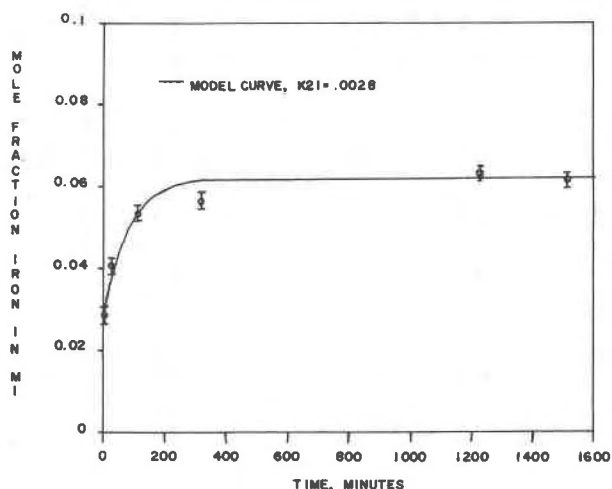


Fig. 4. Disordering with time at 700°C, Sample HC.

reported. This rather reducing atmosphere should be within the stability field of pyroxene, and is similar, at the temperatures investigated, to the iron-wüstite buffer (Muan and Osborn, 1965). Because lower temperature runs were planned for TZ runs than HC, all TZ samples were heated in atmospheres of approximately 60% CO<sub>2</sub>, such that 600°C samples would not be in the graphite stability field found in the more reducing mixture. Oxygen fugacities reported in Table 2 are from the table of Prunier (1978). The influence of other gas mixtures on the disordering rate will be reported in another paper.

The site occupancy is calculated by multiplying the fraction of Fe in the M1 site by  $2\text{Fe}^{2+}/(\text{Fe}^{2+} + \text{Mg}^{2+})$  to obtain the mole fraction on M1. Use of this factor ignores the presence of other cations such as Ca and Al, present only in minor amounts and having an unknown effect in any case (but see Snellenburg (1975) for a discussion of possible blocking effects of minor ions on equilibrium distributions). Equilibrium values of  $X(\text{FeM1})$  are not bracketed in this study, but multiple samples were used to verify that no further disordering was occurring. The rate was also monitored with the shorter runs to ensure that equilibrium runs were sufficiently long to provide steady state values. Further work on equilibrium distributions is underway.

While Virgo and Hafner (1969) were able to estimate only disordering rates from one sample already indistinguishable (within limits of error) from equilibrium at 1000°C and several samples at 500°C (for which the equilibrium determination may be suspect,

as discussed below), Table 2 has many nonequilibrium samples at various temperatures. For all but one sample-temperature combination, a reasonably steady increase in disorder is found with isothermal heating, and these will be analyzed with the Mueller rate model.

For sample HC at 800°C, however, a disconcerting maximum occurs at about 100 minutes, followed by a slow dropoff. Within 95 percent confidence limits this is a real effect. It is believed that it results from the breakdown of minor anthophyllite impurities.

Most of the data can be fitted reasonably to curves calculated with equation (5), although conservative analysis of errors does not allow a test of the validity of the model (Figs. 3, 4). In most cases, calculations were performed using an average of the longest run samples as the assumed equilibrium value. The initial value was obtained from the minimum-time heated sample, and each intermediate sample was used for a separate determination of  $K(21)$ . Sample numbers used for equilibrium are indicated in Table 2 with an "e". For the 800°C data on sample HC, the observed maximum in disorder is used as the apparent short-term equilibrium value, and the unheated sample average as the initial value; both procedures introduce some uncertainty, but the resulting rate constant agrees with extrapolations from lower temperatures (Fig. 5). Data are sparse for sample TZ at 800°C because of the rapidity of disordering; sample 118 could be regarded as already at equilibrium, thus providing a minimum value for  $K(21)$ .

Kinetic data are summarized in Table 3, and illustrated in Figure 5, which is a plot of  $\log K(21)$  against reciprocal temperature for both samples. Error bars are derived from the ten determinations of  $K(21)$  at 700°C for sample TZ. The standard deviation of this sample is 0.0074, or 50 percent of the value of  $K(21)$ , and assumes that initial and equilibrium values of  $X(\text{FeM1})$  are accurate. The logarithmic transformation causes the error bars to appear off-center. Linear least square fits to the data also are shown. Activation energy  $E(a)$  is given by the Arrhenius relation,

$$K(21) = A \exp [-E(a)/RT] \quad (8)$$

where  $A$  will not be strongly dependent on temperature if the diffusion mechanism remains constant. The slope of the line times the gas constant  $R$  gives 254 and 260 kJ/mole (60.7 and 62.2 kcal/mole) as the activation energy for samples TZ and HC respectively. Linear fits to the data are consistent with a single exchange mechanism at all temperatures in-

Table 3. Summary of rate constants for disordering

Sample	T <sup>o</sup> K	Avg. K(21)	lnK(21)
TZ	873	$7.41 \times 10^{-4}$	-7.21
TZ	973	$1.47 \times 10^{-2}$	-4.22
TZ	1023	$1.77 \times 10^{-1}$	-1.73
TZ	1073	$4.06 \times 10^{-1}$	-0.90
HC	973	$2.81 \times 10^{-3}$	-5.87
HC	1023	$1.18 \times 10^{-2}$	-4.44
HC	1073	$5.66 \times 10^{-2}$	-2.87

vestigated, within limits of data scatter. The equal slopes of the two lines suggest that the same mechanism is also operative in both samples. Reasons for the difference in rate are probably compositional. It is certainly worth noting that Seifert and Virgo (1975) arrived at an activation energy of 230 kJ/mole for disordering of anthophyllite which suggests that similar mechanisms are operative in this double-chain silicate.

There are many ramifications to these rate data. It is convenient to define a characteristic time  $t(c) = 1/K(21)$ , (Mueller, 1969) which is the approximate time required to reach equilibrium at a given temperature, as may be verified on the model curves in Figures 3 and 4. The extrapolated  $t(c)$  at 500°C is 98 days (sample TZ) or 1065 days (sample HC). The author is unaware of any experimental run at 500°C longer than 21 days; equilibrium determination at these low temperatures should be done either with adequately long runs on samples with known rates, or by bracketing the equilibrium value with both ordering and disordering runs.

Conversely, the rates at high temperatures are extremely rapid. The characteristic time at 900°C for sample TZ is 12 seconds, and for sample HC is 1.5 minutes; at 1000°C, times are 1.5 and 11 seconds respectively. Even the best quenching procedures are unlikely to capture accurate equilibrium values at these temperatures; this provides an explanation for the "constant" level of disorder at 1000°C and above found by Virgo and Hafner (1969). As noted by Anderson (1970), the fastest possible quench from high temperatures (near melting) has a likely mean diffusion length of 2–5 nm before diffusion is frozen out, so that significant local rearrangements can occur.

To interpret the data of Khristoforov *et al.* (1974), one must first establish probable limits of error. They quote  $\pm 0.01$  for mole fraction of iron in one site, presumably based on prior runs on one sample. No confidence limits are given, nor is it explained whether it

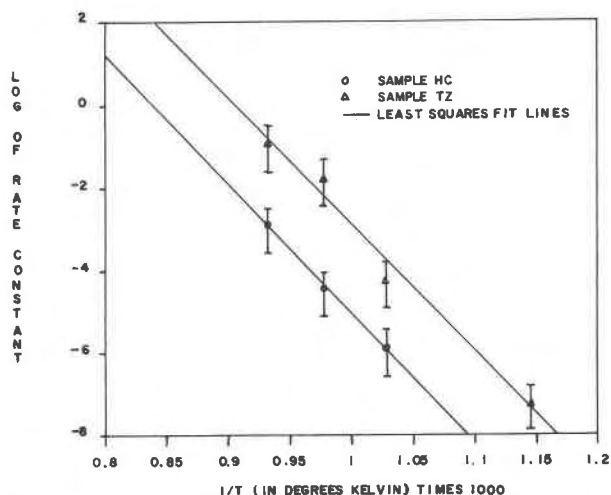


Fig. 5. Variation of rate constants  $K(21)$  with temperature. Linear fit suggests that the same disordering mechanism is found at all temperatures investigated, and that extrapolation to lower temperatures may be valid.

is a sample standard deviation or subjective error estimate. In any case, all their 700°C data have  $X(\text{FeM1}) = 0.373 \pm 0.01$  (for a sample with  $X = 0.57$ , after recalculation to conform to the method of Saxena and Ghose, 1971), which is not surprising with a minimum run time of 14 hours. No kinetic analysis is possible. Virgo and Hafner arrived at an almost identical value  $X(\text{FeM1}) = 0.372$  for their sample 3209, which had the same approximate composition,  $X = 0.574$ .

At 500°C, Khristoforov *et al.* had a maximum run duration of 240 hours, which may be adequate for determination of equilibrium in their sample, as illustrated by Figure 1, in which the calculated curve is based on an average  $K(21)$  determined from their data. Attempted variation of the assumed equilibrium value does not significantly alter the characteristic time, suggesting that equilibrium was probably achieved. Virgo and Hafner performed ordering and disordering experiments on their sample 3209, with the same approximate bulk composition, but apparently neither set of experimental runs achieved equilibrium. If the equilibrium determination by Khristoforov *et al.* is used with the assumption that all of Virgo and Hafner's 500°C data are for only partially disordered samples, an average  $K(21)$  of  $6.8 \times 10^{-6} \text{ min}^{-1}$  is found. The characteristic time of 102 days is in close agreement with the extrapolated characteristic time of 98 days for sample TZ. On the other hand, the partially disordered samples of Khristofo-



rov *et al.* lead to a characteristic time of 3.4 days, suggesting that Fe/(Fe+Mg) ratios should not be the major control of disordering rates.

At 900°C, the data of Khristoforov *et al.* are all for 1 hour to 168 hours, and appear to define a long-term, increasingly disordered pattern. When all are plotted there is not a consistent increase, but the overall increasing trend seems real, even assuming larger estimates of error. Because their samples were heated in evacuated capsules, different mechanisms of disordering might apply, but it seems more likely that some process other than simple disordering causes the increase. If an average activation energy of 257 kJ/mole is assumed for the Khristoforov *et al.* sample, and the 500°C rate constant calculated above is correct, then the characteristic equilibrium disordering time at 900°C would be 0.35 seconds, suggesting that the scatter might have resulted from quenching procedures.

Equilibrium distribution coefficients are summarized in Table 4; these are averages taken from the "e" samples in Table 2. In order to arrive at an apparent equilibration temperature for unheated samples, some equilibrium model must be adopted. Virgo and Hafner (1969) suggest that  $\Delta G$  (15.27 kJ/mole for their sample 3209) is apparently invariant with temperature; this is even more likely if possibly erroneous results at 1000° and 500°C are not included (leaving 13.85, 14.18, and 13.89 kJ/mole at 600°, 700°, and 800°C, respectively). For both TZ and HC, however,  $\Delta G$  increases as temperature decreases (Table 4) even though TZ is similar in composition to the Virgo and Hafner sample. Possible reasons include impurity effects or the presence of small amounts of Fe<sup>3+</sup> (sample TZ). A similar decrease in the magnitude of  $\Delta G$  with increase in the temperature is also found in many of Saxena and Ghose's pyroxene samples, and by Seifert (1978) in anthophyllite. Until data at more temperatures are available, no firm estimates can be made of  $\Delta S$ , the entropy in excess of ideal Fe-Mg configurational entropy, or of apparent equilibrium temperatures of natural samples. Present data would indicate apparent temperatures of about 470°C for sample HC using equation 6, and  $\Delta S = 17.85$  J/mole K and  $\Delta H = 28.09$  kJ/mole, which were obtained using a least squares fit to free energies calculated with equation 4. If a constant average free energy (invariant with temperature) were used instead, apparent equilibration would be about 220°C, showing the importance of a correct estimate of  $\Delta S$ . In addition, uncertainties are introduced by other effects of heating, including

Table 4. Summary of equilibrium distributions

Sample	T°C	X <sub>FeM1</sub>	K <sub>D</sub>	-RTlnK <sub>D</sub> kJ/mole
TZ	600	0.2480	0.1199	15.39
TZ	700	0.2834	0.1687	14.40
TZ	750	0.2907	0.1864	14.29
TZ	800	0.3164	0.2359	12.89
HC	700	0.0626	0.2672	10.68
HC	750	0.0701	0.3165	9.78
HC	800	0.0770*	0.3666	8.95

\*Distribution at maximum disorder on curve (see text).

annealing of exsolution lamellae and possible reaction with buffering gas mixtures. Minor cation constituents could either partially "block" some sites (Snellenburg, 1975), or affect the Mössbauer spectrum of nearby iron atoms (Dowty and Lindsley, 1973). Accurate estimation of apparent equilibration temperature or cooling rate (Seifert and Virgo, 1975) may be difficult if these factors (and measurement errors) are not properly evaluated. Until low temperature behavior is better understood, it does not appear necessary to invoke a two-step mechanism for ordering kinetics (Mueller, 1970); the activation energies reported here may be consistent with observed natural distributions.

### Conclusions

Orthopyroxene order-disorder has real promise as an indicator of cooling histories. Because activation energies are higher than previously thought, a single Arrhenius equation should allow extrapolation of ordering rates measured in the laboratory to low temperatures and long time spans. If the apparently constant activation energy found for two samples is generally applicable, then only a single rate determination and use of an accurate equilibrium model are required to estimate cooling rates of natural samples.

Rate data of Virgo and Hafner (1969) and of Khristoforov *et al.* (1974), and equilibrium data of Virgo and Hafner (1969) and Saxena and Ghose (1971) may be interpreted as consistent with the new rate data presented here. Further study of equilibria at temperatures of about 500°C, and of excess entropy of ordering, will allow more confident extrapolations to lower temperatures.

### Acknowledgments

Numerous individuals have contributed to my understanding of the problems discussed here. I wish especially to thank Roger G.



Burns, who has given both material support and helpful advice at all stages of this investigation. Discussions with Al Duba, Earle Whipple, Norman Gray, Joseph Chernosky, David Kohlstedt, and David Wones were particularly useful. Excellent and constructive reviews by S.K. Saxena and Eric Dowty are gratefully acknowledged. Financial support has come from the Department of Earth and Planetary Sciences at MIT, from Wellesley College, and from NASA grant NSG 7604 to Roger Burns. Laboratory assistance by Margery Osborne and Jill Karsten is gratefully acknowledged. Samples were kindly provided by Harold Fairbairn.

## References

- Anderson, J.S. (1970) Nonstoichiometric and ordered phases: Thermodynamic considerations. In L. Eyring and M. O'Keefe, Eds., *The Chemistry of Extended Defects in Non-Metallic Solids*, p.1-20. North Holland / American Elsevier, New York.
- Buening, D. K. and Buseck, P. R. (1973) Fe-Mg Lattice Diffusion in Olivine. *Journal of Geophysical Research*, 78, 6852-6862.
- Dowty, E. and Lindsley, D. (1973) Mössbauer spectra of synthetic hedenbergite-ferrosilite pyroxenes. *American Mineralogist*, 58, 850-868.
- Ghose, S. (1965)  $Mg^{2+}$ - $Fe^{2+}$  order in an orthopyroxene,  $Mg_{0.93}Fe_{1.07}Si_2O_6$ . *Zeitschrift für Kristallographie*, 122, 81-99.
- Grover, J.E., 1980, Thermodynamics of Pyroxenes. In C.T. Pre-witt, Ed., *Pyroxenes. Reviews in Mineralogy*, 7, 341-417.
- Johnston, J.H. (1979) A Mössbauer spectroscopic study of the cooling history of hypersthene from selected members of the Taupo Pumice formation, New Zealand. *Mineralogical Magazine*, 43, 279-285.
- Khisina, N.R., Belokoneva, E.L., Simonov, M.A., Ivanov, V.I., and Makarov, E.S. (1976)  $Fe^{2+}Mg^{2+}$  Ordering on orthopyroxenes of "Luna 20" and their thermal history. *Geokhimiia*, 1612-1623.
- Khristoforov, K.K., Nikitina, L.P., Krizhanskii, L.M. and Eki-mov, S.P. (1974) Kinetics of iron (2+) ion disordering in structure of rhombic pyroxenes. *Doklady Akademia Nauk SSSR*, 214, 909-912 (transl. *Doklady Earth Science Sections*, 214, 165-167, 1975).
- Muan, A., and Osborn, E.F. (1965) *Phase Equilibria Among Oxides in Steelmaking*. Addison-Wesley, Reading, Massachusetts.
- Mueller, R.F. (1967) Model for order-disorder kinetics in certain quasi-binary crystals of continuously variable composition. *Journal of Physics and Chemistry of Solids*, 28, 2239-2243.
- Mueller, R.F. (1969) Kinetics and thermodynamics of intracrystalline distributions. *Mineralogical Society of America Special Paper* 2, 83-93.
- Mueller, R.F. (1970) Two-step mechanism for order-disorder kinetics in silicates. *American Mineralogist*, 55, 1210-1218.
- Nafziger, R., Ulmer, G., and Woermann, E. (1971) Gaseous buffering for the control of oxygen fugacity at one atmosphere. In G.C. Ulmer, Ed., *Research Techniques for High Pressure and High Temperature*, p.9-41. Springer-Verlag, New York.
- Navrotsky, A. (1971) The intracrystalline cation distribution and the thermodynamics of solid solution formation in the system  $FeSiO_3$ - $MgSiO_3$ . *American Mineralogist*, 56, 201-211.
- Prunier, A.R. (1978) Calculation of Temperature-Oxygen Fugacity Tables for  $H_2$ - $CO_2$  Gas Mixtures at One Atmosphere Total Pressure, and An Investigation of the Zoisite-Clinozoisite Transition. M.S. Thesis, Virginia Polytechnic Institute and State University, Blacksburg, Virginia.
- Sack, R.O., (1980) Some constraints on the thermodynamic mixing properties of Fe-Mg orthopyroxenes and olivines. *Contributions to Mineralogy and Petrology*, 71, 257-269.
- Saxena, S.K. (1973) *Thermodynamics of Rock-Forming Crystalline Solutions*. Springer-Verlag, New York.
- Saxena, S.K. and Ghose, S. (1971)  $Mg^{2+}$ - $Fe^{2+}$  order-disorder and the thermodynamics of the orthopyroxene-crystalline solution. *American Mineralogist*, 56, 532-559.
- Seifert, F.A. (1978) Equilibrium  $Mg$ - $Fe^{2+}$  cation distribution in anthophyllite. *American Journal of Science*, 278, 1323-1333.
- Seifert, F.A. and Virgo, D. (1974) Temperature dependence of intracrystalline  $Fe^{2+}$ - $Mg$  distribution in natural anthophyllite. *Carnegie Institution of Washington Year Book*, 73, 405-411.
- Seifert, F.A. and Virgo, D. (1975) Kinetics of the  $Fe^{2+}$ - $Mg$ , order-disorder reaction in anthophyllites: Quantitative cooling rates. *Science*, 188, 1107-1109.
- Snellenburg, J.W. (1975) Computer simulation of the distribution of octahedral cations in orthopyroxenes. *American Mineralogist*, 60, 441-447.
- Stone, A.J., Augard, H.J., and Fenger, J. (1971) MOSSPEC: A program for resolving Mossbauer spectra. Danish Atomic Energy Commission Risoe Research Establishment, Denmark. Report RISO-M-1348, 42 p.
- Thompson, J.B., Jr. (1969) Chemical reactions in crystals. *American Mineralogist*, 54, 341-375.
- Thompson, J.B., Jr. (1970) Chemical reactions in crystals: corrections and clarification. *American Mineralogist*, 55, 528-532.
- Virgo, D. and Hafner, S.S. (1969)  $Fe^{2+}$ - $Mg$  disorder in heated orthopyroxenes. *Mineralogical Society of America Special Paper* 2, 67-81.
- Virgo, D. and Hafner, S.S. (1970)  $Fe^{2+}$ ,  $Mg$  order-disorder in natural orthopyroxenes. *American Mineralogist*, 55, 201-223.

*Manuscript received, November 18, 1980;  
accepted for publication, May 20, 1981.*